Journal of Hazardous Materials 180 (2010) 332–339

Contents lists available at ScienceDirect

Journal of Hazardous Materials

journal homepage: www.elsevier.com/locate/jhazmat

Modeling of LNG spills into trenches

Filippo Gavelli [a,*], Melissa K. Chernovsky [a], Edward Bullister [b], Harri K. Kytomaa [c]

[a] Exponent, Inc., 17000 Science Drive, Suite 200, Bowie, MD 20715, USA
[b] Cambridge Technology Development, Inc., 20 Rolling Lane, Weston, MA 02493, USA
[c] Exponent, Inc., 9 Strathmore Road, Natick, MA 01760, USA

ARTICLE INFO

Article history:
Received 11 June 2009
Received in revised form 9 April 2010
Accepted 12 April 2010
Available online 24 April 2010

Keywords:
LNG
CFD modeling
Vapor dispersion
Hazard distance
Trench

ABSTRACT

A new method for the analysis of LNG spills into trenches has been developed to quantify vapor dispersion hazard distances. The model uses three steps to capture the behavior of an LNG spill into a trench. The first is to analytically calculate the evolving LNG flow, the second to calculate the vaporization rate along the trench, and the third is to calculate the dispersion of the vapors using a CFD model that has been validated for this application in the presence of complex geometries. This paper presents case studies that show the effect of wind perpendicular and parallel to the large aspect ratio trenches on vapor dispersion. The case studies also demonstrate the effect of complex terrain and obstacles such as vapor fences on vapor dispersion. The simulations show that wind direction relative to the trench has a significant effect on cloud shape, height, and maximum downwind distance. The addition of vapor fences to mitigate vapor dispersion hazards from an LNG spill into the LNG containment trench is shown to be effective.

1. Introduction and motivation

US Federal regulations for the siting of onshore LNG receiving terminals require that all LNG transfer systems be provided with means to collect a spill and direct it to a containment location. This is generally accomplished by running trenches underneath or adjacent to piping and equipment areas and by sizing and sloping the trenches so that they can collect a design spill and direct it to a properly sized LNG containment sump, where it will slowly evaporate. However, some of the LNG spilled into the trench will vaporize as it flows towards the containment sump. The vapor cloud thus formed along the trench will be dispersed by the wind in the same manner as the vapor cloud generated by a spill into a containment area.

Current US federal regulations do not explicitly require the vapor cloud dispersion from an LNG trench to be modeled, nor do they provide any guidance for performing such analysis. However, the LNG trenches often run closer to the property line than the containment sumps, and therefore the potential for dispersion of a flammable vapor cloud beyond the terminal boundaries cannot be excluded. For this reason, the US Federal Energy Regulatory Commission (FERC) has been requesting LNG receiving terminal applicants to demonstrate that the vapor cloud generated by the LNG vaporization along the trenches will dissipate to below 50% of the lower flammable limit (½-LFL) within the terminal boundaries [1].

There currently is no standardized procedure for the calculation of vapor dispersion hazard distances for LNG spills into trenches. DEGADIS, the modeling tool that is often used for vapor dispersion calculations from impoundment areas, is limited in applicability to LNG pools of small aspect ratio (up to approximately 4:1), whereas trenches often exceed aspect ratios of 100:1. Therefore, DEGADIS and other similar integral models cannot be applied to vapor dispersion calculations from LNG spills into trenches, and attempts to use DEGADIS for these scenarios have not been received favorably by the authorities.

On the other hand, models developed for the simulation of gaseous releases from long and narrow sources (e.g., CALINE3 which was developed to study pollution from highways) are limited in their applicability to passive releases and cannot accurately predict dense gas releases such as LNG vapor from spills into trenches. Additionally, there is currently no reliable model to quantify the LNG vapor source term from LNG flow into long and narrow trenches. Therefore, in order to provide the LNG industry with means to quantify LNG vapor dispersion hazard distances from these scenarios, a new approach has been developed. The present modeling approach consists of a spreadsheet-based hydraulic model to calculate the time dependent LNG flow and vapor generation along an open trench, from the spill location to the containment sump, coupled with a CFD model to perform the vapor dispersion calculations. The hydraulic model takes into account variables such as the spill flow rate and duration; the dimensions of the channel (width, depth, shape, and slope); the composition

* Corresponding author. Current address: Gexcon US, Inc., 7735 Old Georgetown Rd, Suite 1010, Bethesda, Maryland 20814 USA. Tel.: +1 301 915 9925; fax: +1 301 656 2953.
E-mail address: fgavelli@gexcon.com (F. Gavelli).

0304-3894/$ – see front matter © 2010 Elsevier B.V. All rights reserved.
doi:10.1016/j.jhazmat.2010.04.035

Nomenclature

k	thermal conductivity (W/m K)
L	characteristic length (m)
n	Manning friction coefficient (s/m$^{1/3}$)
$q''(x, t)$	heat flux per unit area (W/m^2)
R_h	hydraulic radius (m)
S_0	trench slope
$t_0(x)$	time of first wetting (s)
T_s	trench surface temperature (K)
T_i	initial (ambient) temperature (K)
U	average speed (m/s)
V	speed of the leading edge (m/s)

Greek symbols

α	thermal diffusivity (m^2/s)
τ	characteristic time (s)

of the walls (e.g., regular or aerated concrete); and ambient conditions (air and ground temperatures). The output from the hydraulic model is a time- and space-dependent rate of LNG vapor generation along the trench. The LNG vapor generation rate provides the vapor source term for the CFD model. The CFD model calculates the dispersion of the LNG vapor cloud as a result of wind–vapor interaction, as well as heat transfer from the air and ground to the vapor cloud; therefore, environmental conditions such as atmospheric stability, wind speed and direction, air temperature and humidity, and ground temperature can all be varied to determine their impact on the LNG vapor cloud dispersion. The CFD model inherently accounts for the effects of non-uniform terrain and infrastructure (e.g., LNG storage tanks, buildings, elevated trench, levees), and can evaluate the effect of vapor barriers on cloud dispersion.

The purpose of this paper is to present a reliable method to quantify and bound LNG vapor dispersion hazard distances for regulatory purposes. The method makes several conservative assumptions, particularly in the derivation of the LNG vapor source term. More sophisticated models could be used to predict the flow and vaporization of LNG along the trench (for example, by numerical integration of the shallow water equations). However, in the absence of experimental data that can be used to evaluate these models, their use for regulatory purposes would be difficult to justify. The following sections describe the conservative method developed by the authors and its application to a set of case studies.

2. Physical scenario

The scenario for an LNG spill into a trench is based on a constant-flow leak from transfer piping (typically, either the unloading line or the sendout line), with a steady flow rate of LNG into a trench that is designed to collect the spill and direct it towards a containment sump. The LNG spill flow rate and duration are typically determined according to US federal regulations [2] (for example, a 10 min spill through the largest non-welded pipe connection in the line). The LNG spilled into the trench follows the slope of the trench towards the LNG containment sump. The LNG flow characteristics are determined by a balance of gravity and frictional forces. Heat transfer from the trench walls and floor causes vaporization of the LNG along the trench.

As LNG begins to flow into the trench, the liquid depth in the trench progressively rises. Additionally, as LNG first comes in contact with the trench floor and walls at a given location, heat transfer from the trench surface contributes to vaporizing the LNG. Very high rates of heat transfer occur when a surface first comes into contact with LNG, but the heat transfer decreases rapidly as the trench floor and walls cool down.

3. Model approach

The approach to the physical scenario of an LNG spill into a trench consists of three steps:

(1) The flow of liquid LNG in the trench is first calculated with an algebraic hydraulic model.
(2) The time varying rate of vaporization along an open trench is calculated from the hydraulic model as the spill progresses from the initial spill location to the containment sump.
(3) The time varying vapor generation is input into a validated CFD model to perform the vapor dispersion calculations.

In order to treat the LNG trench flow analytically, some simplifying assumptions are made. These are discussed in the following sections.

3.1. Source term models

3.1.1. Hydraulic model

The hydraulic model calculates the maximum depth of LNG in the trench, based on the channel shape, slope and dimensions. The assumption is made that LNG flow along the trench is constant and equal to the steady-state flow as calculated using Manning's equation [3] for open channel flow:

$$U = \frac{R_h^{2/3} S_0^{1/2}}{n} \quad (1)$$

where U is the average liquid speed in the trench in m/s, R_h is the hydraulic radius in m (for an open channel, the hydraulic radius is equal to the cross-sectional area of the flow divided by the wetted perimeter [3]), S_0 is the slope of the trench in m/m, and n is the coefficient of friction for LNG flow over the channel floor and walls, which has units of s/m$^{1/3}$. The coefficient of friction assumes liquid-to-substrate contact. This is a reasonable assumption even for a cryogenic liquid because film boiling, which would result in a much smaller friction coefficient, has been observed experimentally to last only a very limited time when LNG is in contact with poorly conducting substrates [4]. Therefore, only a short segment of the wetted trench could be experiencing reduced friction at any given time. In the absence of data on the coefficient of friction for LNG on various substrates, the values for water flow are chosen, as listed in Table 1.

The assumption that the LNG depth in the trench instantaneously reaches the steady-state value, instead of growing over time, is conservative, as it provides a higher area for heat transfer to the LNG and consequently a higher vaporization rate. The choice of the steady-state flow conditions to calculate the speed of the LNG front along the trench is also conservative, as higher liquid depth results in higher front speed. This corresponds to a faster rate of surface wetting and consequently, a higher rate of LNG vapor generation from the trench. The open channel flow equation applies to steady-state flow of non-boiling liquids, in which case the mass flow rate is constant along the channel. In the case of LNG flow, instead, heat transfer from the walls leads to vaporization of the flowing liquid, which results in a decreasing mass flow rate along the trench. The decrease in mass flow rate is not accounted for

Table 1
Values of the Manning friction coefficient, n for water on typical trench substrates.

	Concrete	Asphalt	Gravel
Friction coefficient, n (s/m$^{1/3}$)	0.012	0.016	0.025

Table 2
Thermophysical properties of typical trench substrates.

	Concrete	Aerated concrete
Thermal conductivity, k (W/m K)	1.45	0.28
Thermal diffusivity, α (m^2/s)	4.9e-7	2.6e-7

in the presented hydraulic model. As a consequence, the model overestimates the wetted trench area and, proportionally, the LNG vaporization rate. Similarly to the other approximations previously discussed, this is a conservative choice which increases public safety.

3.1.2. Heat transfer – vaporization model

As LNG flows along the trench and wets the channel, heat transfer occurs between the warmer walls and the colder LNG; as a result, the trench surfaces become progressively colder while the LNG boils off. Heat transfer between the trench and the LNG is extremely difficult to predict accurately. Initially, heat transfer is expected to occur in the film boiling regime, but as the trench surface becomes colder, the heat transfer mode will transition to nucleate boiling, which has substantially different characteristics; additionally, the rate of heat transfer will be a function of the channel geometry (e.g., horizontal, inclined or vertical walls) and will vary along the wetted perimeter. In order to develop a model that is acceptable for regulatory purposes, the heat flux from the trench channel surface to the LNG is calculated using the semi-infinite solid model with an imposed temperature boundary condition at the solid wall surface [5]:

$$q''(x,t) = k\frac{T_i - T_s}{\sqrt{\pi\alpha(t - t_0(x))}} \quad \text{if } t > t_0(x) \tag{2}$$

where: $q''(x, t)$ is the heat flux per unit area of contact between the trench walls and LNG, as a function of position and time in W/m^2; k and α are thermophysical properties of the trench substrate in W/m K and m^2/s, respectively; T_s and T_i are, respectively, the imposed trench surface and initial (ambient) temperatures in K; $t_0(x)$ is the time in s (from the beginning of the spill) at which the trench floor and walls at distance x from the spill origin are first wetted.

The most common trench substrates are concrete or aerated concrete. Approximate values for the thermophysical properties of these materials are given in Table 2.

The heat flux calculated from Eq. (2) is unequivocally the largest heat flux that can be transferred from the substrate to the LNG, as it assumes that the substrate surface is equal to the temperature of the LNG. Once again, this is a conservative assumption that overpredicts the evaporation rate.

Heat transfer from the trench to the LNG causes vaporization of the saturated liquid. The flux of LNG vapor into the ambient is a function of time, as well as of the position along the trench proportional to the local heat transfer rate. At any given position x, the maximum LNG vapor generation occurs when the LNG front reaches position x; the vapor generation rate then decreases rapidly, as the trench walls cool down (Fig. 1).

3.1.3. Sensitivity to source term model parameters

The LNG vapor source term obtained from the trench flow and heat transfer models described above is a function of the trench substrate material. In fact, the substrate affects both the LNG flow along the trench, by means of the coefficient of friction, as well as the vapor generation rate, by means of the thermal conductivity and diffusivity. In general, a smoother substrate will result in a faster LNG front speed, which in turn will increase the rate at which the trench is wetted. However, a faster LNG front has a thinner liquid depth, which reduces the heat transfer area. The net

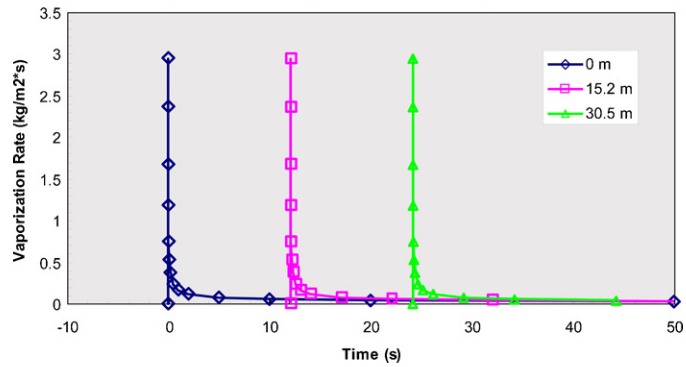

Fig. 1. Example of LNG vaporization rate per unit area as a function of time, at different positions along a trench relative to the spill location at 0 m.

result for practical scenarios is that a faster LNG flow will result in slightly longer vapor cloud dispersion distances. The effect of thermal properties is much more noticeable; with reference to the data in Table 2, the vapor generation rate for the concrete-lined trench is approximately 3.8 times that of an aerated concrete trench.

The analysis presented in this paper computes the rate of evaporation of LNG based on a hydraulic calculation, in which the liquid is not depleted by the evaporation. As a result, the walls of the trench are predicted to be wetted to a greater depth and by a faster spreading front than in an actual scenario. This causes the calculated vapor source to be larger than in reality.

The degree of overestimation of the vapor source and its impact on vapor dispersion distances can be estimated by quantifying the rate of evaporation over the wetted trench, and comparing it to the LNG spill rate at the source. If the rate of evaporation makes up a significant fraction of the spill rate, the loss of liquid to vapor can be viewed as a loss of liquid that results in a smaller net spill rate. This in turn decreases both the front speed and the depth of the flowing LNG. As the LNG evaporates, the LNG depth will equilibrate over the wetted length of the trench as long as the flow is subcritical. In the case studies presented here (see Section 4), the Froude number is 0.59 and the flow is indeed subcritical, which allows waves to travel upstream to equilibrate the depth over the length of the trench.

The cumulative amount of evaporated LNG as it flows along the trench and the total rate of evaporation are shown in Figs. 2 and 3 for the case study No. 1 (see Section 4.1 below). The highest rate of evaporation (7.55 kg/s) occurs at approximately 95 s and amounts to only 1.60% of the total spill rate (475 kg/s). Therefore, while the spill is expected to generate a large volume of vapor and visible fog,

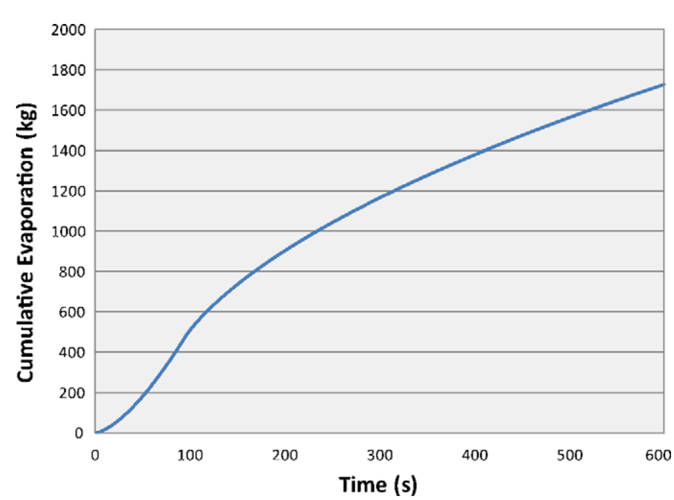

Fig. 2. Example of the cumulative evaporation mass loss as a function of time.

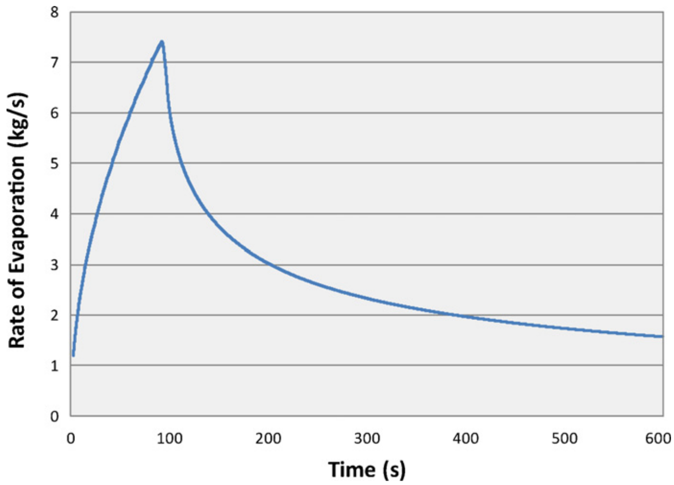

Fig. 3. Example of the total mass loss rate as a function of time.

the hydraulics of the LNG flow in the trench is largely unaffected by evaporation.

For the given trench geometry, a decrease of 1.60% in the net spill rate results in a 1.11% decrease in LNG depth and a 0.49% decrease in the LNG speed in the trench. The change in depth corresponds to a 0.37% change in the wetted perimeter of the channel. These two effects are cumulative and result in a decreased rate of wall wetting of 1.48% (1.11% + 0.37%), and a corresponding decrease in evaporation rate of 1.48%.

The vapor cloud that is formed by a long LNG trench with a perpendicular wind travels furthest near the leading edge, where the heat transfer rate from the concrete is highest, with shorter vapor dispersion distances where the trench walls have been wetted for a longer time. The width of this longer cloud derives from the speed of the leading edge, V, and the characteristic time, τ, it takes for the walls to cool down. If the depth of the flowing LNG remains the same, while the speed V is decreased, this decreases the width of the longer cloud. All else being equal, the vapor dispersion distance is expected to scale linearly with the characteristic length, L, of the trench ($L = V\tau$). Conversely, for a fixed L, if the wetted perimeter of the trench is decreased, the vapor dispersion distance is also expected to scale linearly with the wetter perimeter. It follows therefore that the combined effects of the lesser speed and depth of the spill will result in a decrease of the vapor dispersion distance of 1.48%.

At the source of the spill, where the LNG comes in contact with the trench floor, it will form a thin layer of fast moving (supercritical) liquid that moves radially from the point of contact. This fast moving radial flow then transitions into a channel flow in a complex three-dimensional manner that involves the formation of a hydraulic jump around the source, much like water hitting the kitchen sink. The flow is subcritical downstream of the hydraulic jump and assumes the conditions that are represented by the Manning equation. Near the source, where the flow is locally faster than is predicted by the Manning equation, the rate of evaporation is limited by thermal conduction in the substrate only, so flow speed or turbulence are not expected to have any influence.

At the leading edge, the flowing LNG is expected to exhibit an increased level of turbulence in part due to the vigorous evaporation. While this will increase local flow drag, it will have little to no effect on the rate of evaporation as the rate of evaporation is primarily limited by how much heat the substrate can conduct to the liquid.

If a spill originates downstream of the uphill endpoint of a trench or it tees with another trench feeding into the same downstream LNG collection sump, some of the flowing liquid will move uphill. The liquid that moves uphill will form a pool that will become largely stagnant, with zero depth at its furthest point. A measure of the distance and the surface area that is wetted uphill of the spill can be hydrostatically estimated from the Manning depth and the channel inclination. For the calculations that are presented in this paper, the spill originated at the enclosed end point of the channel. However, if the same spill had originated in a channel downstream of the endpoint, considering an uphill continuation of the channel presented in this paper with the same inclination (0.0011 m/m), the uphill distance that would be wetted would be 422 m, which is 352% of the length of the 120 m channel downstream of the spill origin. The corresponding wetted area is 293% of the total wetted area of the channel downstream of the origin. The uphill aspect of the analysis can be addressed in the same manner as the downhill side. The speed of uphill spreading will generally be smaller than on the downhill side, and can therefore be considered conservatively using the Manning spreading speed.

3.2. Vapor dispersion model

The time- and space-dependent LNG vaporization rate obtained above provides the LNG vapor source term for the CFD model, which then calculates the vapor cloud dispersion. The vapor dispersion calculations presented in this paper were performed using a commercial CFD code, Fluent® [6]. Other CFD programs can also be used for the present application, provided they can be demonstrated to predict dense gas dispersion accurately.

Before a CFD model can be used for LNG vapor dispersion simulations, it must be compared against relevant experimental data, to ensure that the model's predictions are sufficiently accurate. The authors have performed two such studies. One test was performed to demonstrate that Fluent could accurately predict the dispersion of an LNG vapor cloud over flat terrain [7,8]. The Burro series [9] of LNG spill tests represents the benchmark experimental data for a scenario in which vapor cloud dispersion is not affected by obstacles, such as buildings, impoundments or other barriers. When compared to the Burro 8 test, the Fluent results were conservative, over predicting the maximum distance to LFL by approximately 13%. In addition, Fluent has been compared against experimental data for the dispersion of LNG vapor cloud into complex geometries [10]. When considering spills into an impoundment, as opposed to spills over water or flat terrain, it is important to consider the effect of the impoundment walls and the LNG storage tank or process equipment within the impoundment, on vapor dispersion and mixing. The Falcon test series [11] of LNG spills into impoundments represents the benchmark experimental data for this type of scenario. The statistical analysis of the Fluent simulation of the Falcon tests has been submitted for peer-reviewed publication.

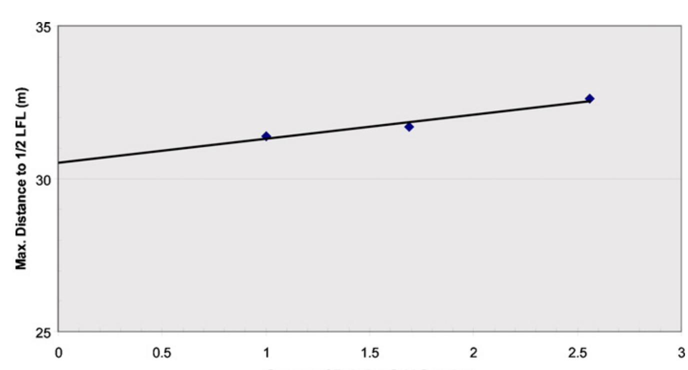

Fig. 4. Example of grid refinement results and Richardson extrapolation.

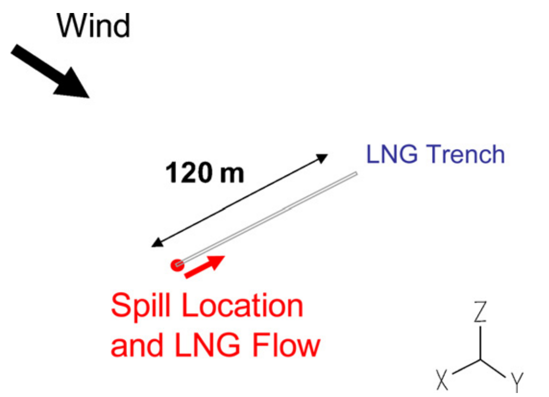

Fig. 5. Trench layout, LNG spill location and flow direction for case study No. 1.

3.2.1. Turbulence model and ambient conditions

A critical component of a CFD model of atmospheric dispersion is the selection of the wind velocity, temperature, and turbulence profiles. In real-life, all these quantities vary with height (for example, wind speed increases with elevation). Therefore, the CFD model needs to reflect this variability as closely as possible. Additionally, a careful selection of the turbulence model is necessary to ensure a consistent propagation of the inlet boundary conditions throughout the computational domain, prior to the injection of the LNG vapors. This avoids situations where, for example, the wind profile changes from the inlet to the outlet boundary, potentially resulting in different cloud dispersion as the location of the boundaries is varied. Based on prior validation work performed by the authors, the realizable k–ε turbulence model [12] was determined to be accurate for this type of analysis. When vapor dispersion simulations are performed for regulatory purposes, the ambient conditions (temperature, wind speed and atmospheric stability) to be used are typically specified by the regulations in order to provide worst-case results. For example, US federal regulations require a wind speed of 2.01 m/s at 10 m elevation and stable atmosphere (Pasquill-Gifford class "F") for hazard distance calculations [13]. For other applications, the modeler should determine whether similar requirements exist, or select values that result in conservative vapor dispersion distances. Once the reference temperature, wind speed and atmospheric stability class are specified, vertical profiles of wind speed, temperature and turbulence parameters can be calculated from the Monin–Obukhov theory [14].

3.2.2. Computational grid

For any given scenario, the vapor dispersion distances depend to some extent on the size of the computational grid, but as the grid is refined, the results eventually asymptote towards a value that is independent of the grid resolution [15]. A typical approach to determine the "grid independent" vapor dispersion distance for a given scenario is to perform the simulation with progressively smaller grid cells, and then apply the Richardson extrapolation method [16]. The authors followed this approach by performing simulations with three different grid resolutions, with relative spacing ratios on the order of 1, 1.3 and 1.6, respectively. Fig. 4 shows the results of the grid refinement and Richardson extrapolation for the maximum distance to ½-LFL in case study No. 2 (see Section 4.2 below). The maximum distance to ½-LFL decreased only slightly with further grid refinement, which confirms that the chosen grid resolution is adequate for the scenario being modeled. The Richardson extrapolated distance for this example is approximately 30.5 m, or less than 3% shorter than the value predicted by the finest grid simulation.

A non-uniform grid was used to discretize the computational domain. The grid was finest in proximity of the trench and close to the ground, and became progressively more coarse away from the trench and at higher elevations. This allowed the mixing and dispersion of the LNG vapor cloud to be adequately resolved, while limiting the computing resources allocated to portions of the domain unaffected by the LNG spill. The smallest cells measured approximately 1 m in the horizontal direction and 0.1 m in the vertical direction; the largest cells measured up to approximately 12 m horizontally and 20 m vertically.

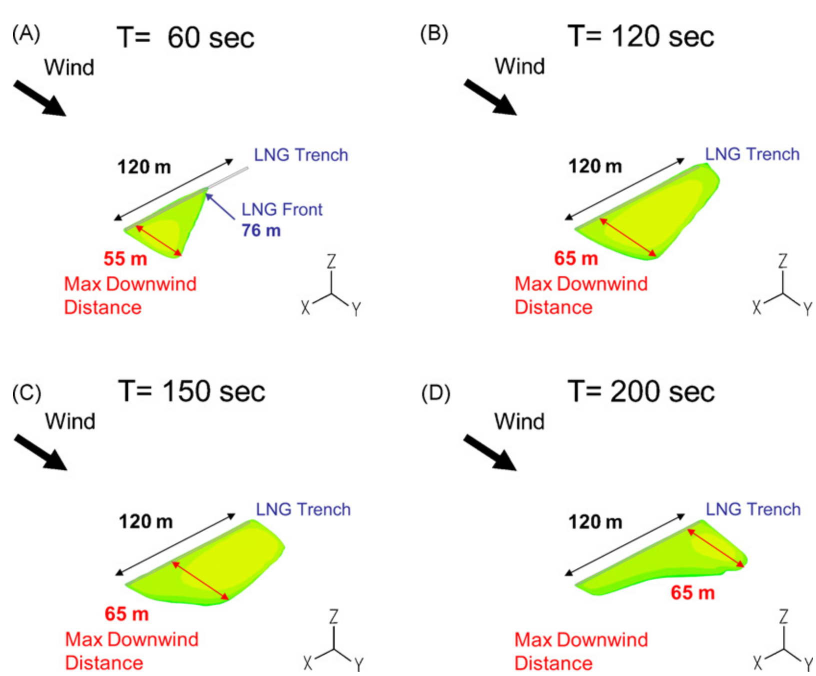

Fig. 6. Case study No. 1. ½-LFL concentration isosurface for the vapor cloud from an LNG spill into a trench, with wind perpendicular to the trench. Simulation times: 60 s (A), 120 s (B), 150 s (C), and 200 s (D).

Table 3
Case study parameters.

Air temperature	20 °C
Relative humidity	50%
Wind speed (at 10 m elevation)	2.01 m/s
Pasquill-Gifford stability class	F
Trench substrate	Aerated concrete
Coefficient of friction	0.012 s/m$^{1/3}$
Spill mass flow rate	475 kg/s
Spill volumetric flow rate	1.08 m^3/s
Spill duration	10 min

4. Case studies

The analysis presented in this paper represents a generic solution method for simulation of vapor dispersion from LNG spills into long and narrow trenches in various configurations. A three-dimensional simulation provides the ability to consider the effect of enhanced mixing due to impoundment walls and the LNG storage tank or process equipment on vapor dispersion distances. The uneven terrain of a LNG terminal, such as ditches, levees, flood walls, retaining walls, elevated pipe racks, etc., can affect dispersion distances either in an adverse or beneficial manner. Barriers with various degrees of permeability can be installed to control the dispersion of the vapor cloud. Site-specific options can be investigated to find solutions that are both cost effective and that provide increased levels of safety.

In the next section case studies are presented to demonstrate the application of the CFD model to scenarios where complex terrain and vapor barriers affect the dispersion of a vapor cloud. All case studies were solved using non-uniform grids and performing the Richardson extrapolation, as discussed in Section 3.2.2. The simulations were run on a single processor, 64-bit Windows machine with a 2.6 GHz CPU; the computational run times were on the order of 12 h per simulation, although the actual times varied from case to case and with grid resolution. The weather conditions, trench, and spill parameters for all case studies are summarized in Table 3.

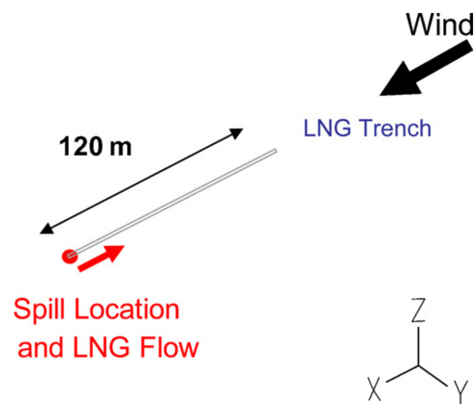

Fig. 7. Trench layout, LNG spill location and flow direction for case study No. 2, without vapor barrier.

4.1. Case study No. 1 – cloud dispersion from a long and narrow trench

The first case study represents vapor dispersion from an LNG spill into a long and narrow trench (approximately 120 m long and 1.8 m wide), with wind blowing perpendicular to the trench. The assumed spill location and the LNG flow direction along the trench are shown in Fig. 5. The terrain is assumed to be mostly flat, with a long depression of 1 m depth that runs parallel to the trench, 95 m downwind of the trench. The trench has uniform, rectangular cross section (1.8 m wide and 1.5 m deep); it is gently sloped (approximately 0.11%) and is lined with aerated concrete. For a 10 min, 475 kg/s LNG spill flow rate, the hydraulic model predicts an LNG depth in the trench of approximately 0.5 m and an LNG flow speed of 1.25 m/s within the trench.

Time series snapshots for ½-LFL concentration surface are shown in Fig. 6, color coded according to the local cloud height above the reference ground level. The generation of LNG vapors along the trench as the spilled liquid flows, is clearly visible when following the time sequence of these images. The ½-LFL concentration vapor cloud extends approximately 65 m downwind of the

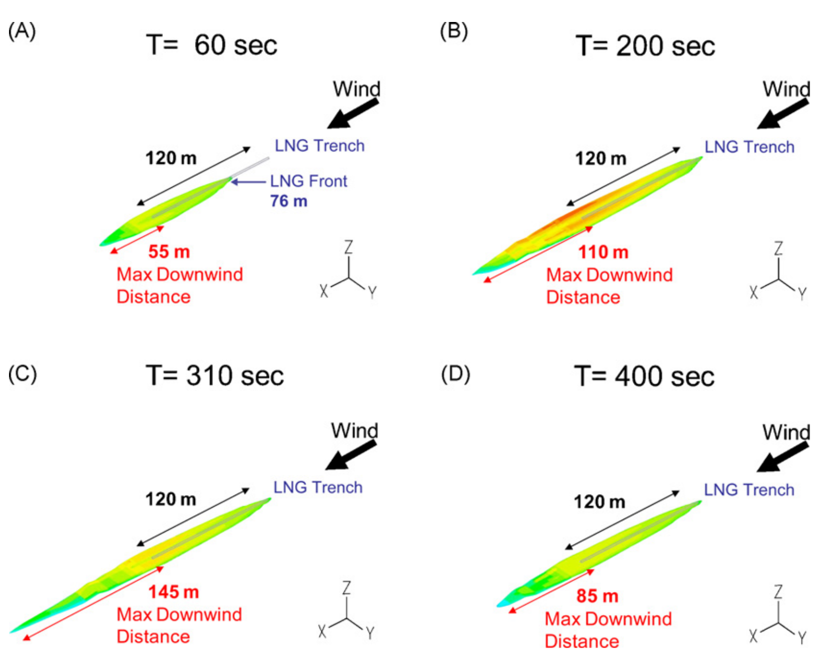

Fig. 8. Case study No. 2. ½-LFL concentration isosurface for the vapor cloud from an LNG spill into a trench, with wind parallel to the trench. Simulation times: 60 s (A), 200 s (B), 310 s (C), and 400 s (D).

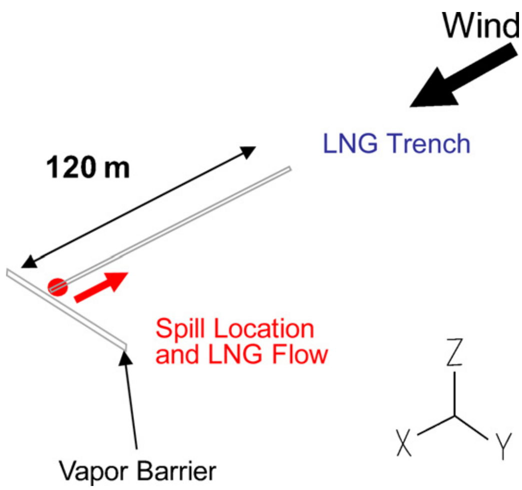

Fig. 9. Trench layout, LNG spill location and flow direction for case study No. 2, with an impermeable vapor barrier perpendicular to the trench.

trench (see Fig. 6B). Fig. 6D shows that the vapor cloud begins to recede well before the 10 min spill duration is complete. This is due to the decreasing heat transfer from the trench walls to the LNG as the trench walls cool down.

4.2. *Case study No. 2 – effect of vapor barrier on cloud dispersion*

In some cases, an LNG spill into a trench with wind blowing parallel to the direction of LNG flow may result in distances to ½-LFL on the order of 100 m or more. This scenario therefore needs to be evaluated to ensure that the ½-LFL cloud concentration does not extend beyond the plant boundaries. An example of LNG vapor cloud dispersion with wind conditions parallel to the trench is shown in Fig. 7. The LNG spill is assumed to occur at the top of the trench and the wind blows parallel to the trench, but in the direction opposite to the flow of LNG. The weather conditions, LNG spill flow rate and trench dimensions are the same as in case study No. 1. In case study No. 2, the terrain is assumed to be flat in the vicinity of the trench, and approximately 25 m downwind of the trench, the terrain is assumed to drop 2 m in depth; additionally, a 2 m high levee is assumed to be located approximately 60 m downwind of the trench.

Fig. 8 shows time series snapshots of the LNG vapor cloud dispersion scenario: the ½-LFL vapor cloud extends beyond the trench location, reaching a maximum downwind dispersion distance of approximately 145 m, or more than twice as far as in the case of wind perpendicular to the trench (see Figs. 8C and 6B, respectively).

If the vapor dispersion distance predicted for a given LNG spill scenario is not in compliance with the regulations, mitigation measures may be taken. For example, US federal regulations [17] allow the use of vapor control systems, such as vapor barriers, to reduce the vapor cloud dispersion distance and allow it to dissipate below ½-LFL within the terminal boundaries. The use of CFD allows the effect of vapor barriers on vapor dispersion to be analyzed and demonstrated.

Fig. 9 shows the location of an impermeable vapor barrier, approximately 65 m wide and 3 m tall, placed in close proximity to the end of the trench and oriented perpendicular to the trench. The effect of the vapor barrier is to partially hold-up the vapor cloud, forcing the heavy vapors to spread crosswind and to rise above the top of the barrier. Even though the cloud is not fully contained by the barrier, increased turbulence and mixing accelerates the dissipation of the smaller cloud that extends beyond the fence (Fig. 10). In the case study presented here, the vapor barrier reduces the downstream vapor dispersion of the ½-LFL concentration vapor cloud to a distance of approximately 30 m from the end of the trench, or approximately 21% of the unimpeded distance.

This result demonstrates the significance of vapor dispersion control strategies that can be employed to mitigate potential vapor dispersion hazards in the event of an LNG spill into transfer piping trenches at an onshore receiving terminal. It must be noted that there is no general rule on the dimensions (height and length) and placement of a vapor barrier, in order for it to be effective in controlling an LNG vapor cloud. Rather, it is a matter of evaluating the site-specific conditions (e.g., spill flow rate, trench dimensions and location with respect to the property line, terrain features) and making an engineering determination that can then be verified, or corrected, using a CFD vapor dispersion model. The selection and placement of a vapor barrier must also take into consideration the

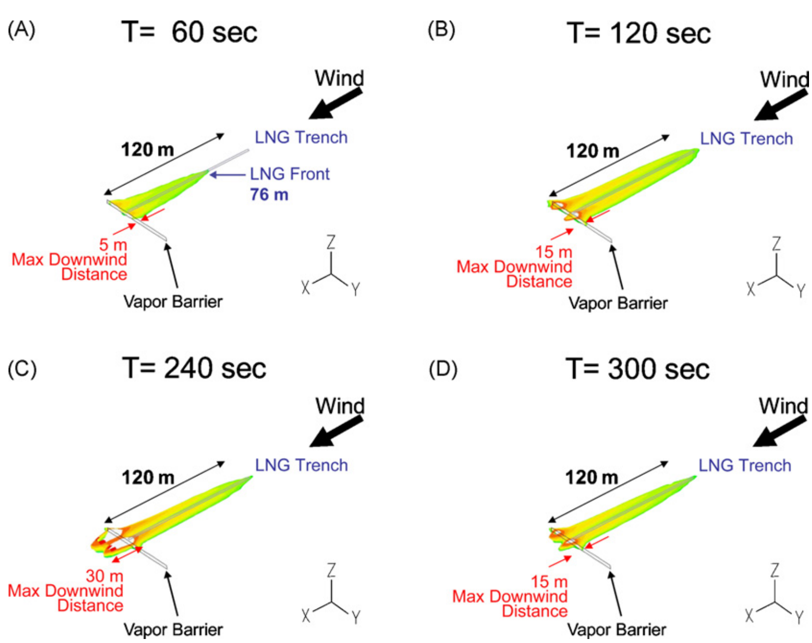

Fig. 10. Case study No. 2. ½-LFL concentration isosurface for the vapor cloud from an LNG spill into a trench, with wind parallel to the trench and including an impermeable vapor barrier perpendicular to the wind. Simulation times: 60 s (A), 120 s (B), 240 s (C), and 300 s (D).

potential for partial confinement of the vapor cloud, which may introduce new hazards.

5. Conclusions

A new method for the analysis of LNG spills into trenches has been developed to quantify vapor dispersion hazard distances for LNG spills into trenches. This method uses a realistic and conservative approach to analyze LNG spills and vapor dispersion. The model consists of three steps to capture the behavior of an LNG spill into a trench. The first is to analytically calculate the evolving LNG flow, the second to calculate the vaporization rate along the trench and the third is to use this time dependant vaporization rate as the vapor source term in a CFD model validated for vapor dispersion in complex geometries.

This solution method has been applied to numerous scenarios, including varied wind speeds and directions with respect to the trench, elevated trenches, complex terrain, and vapor barriers. While existing levees within terminals are helpful to control the vapor cloud, the addition of vapor fences has proven effective, by providing a barrier for vapor hold-up in addition to increased turbulence and mixing, leading to increased vapor dissipation rates and smaller downwind plume distances. Vapor fences can be a cost effective option to meet new regulatory requirements regarding vapor dispersion from LNG containment trenches that out of necessity run in close proximity to property lines. However, the selection and placement of a vapor barrier needs to be done carefully, as additional hazards may be introduced. For example, if vapor barriers are introduced in partially confined areas, it may be necessary to consider the influence of added confinement of the vapor cloud.

References

[1] FERC Information Requests on dockets CP05-396 (10/19/2006), CP05-13 (10/30/2006), CP03-75 (12/14/2006), CP07-35 (10/11/2007), PF07-3 (9/7/2007).
[2] NFPA 59A-2001 Section 2.2.3.5 as referenced by 49 CFR 193.2059.
[3] B.R. Munson, D.F. Young, T.H. Okiishi, Fundamentals of Fluid Mechanics, third ed., John Wiley & Sons, New York, 1998, pp. 652-656.
[4] D.M. Webber, S.E. Gant, M.J. Ivings, S.F. Jagger, LNG Source Term Models for Hazard Analysis: a Review of the State-of-the-Art and an Approach to Model Assessment, Health & Safety Laboratory, March 2009.
[5] F.P. Incropera, D.P. DeWitt, Fundamentals of Heat and Mass Transfer, fourth ed., John Wiley & Sons, New York, 1996, pp. 236–239.
[6] www.fluent.com.
[7] Neptune LNG, DOT Docket No.: USCG-2004-22611, Final Environmental Impact Statement, Section 5 and Appendix I, November 1, 2006.
[8] Northeast Gateway, DOT Docket No.: USCG-2005-22219, Final Environmental Impact Statement, Chapter 5 and Appendix K, October 24, 2006.
[9] R.P. Koopman et al., LLNL/NWC1980 LNG Spill Tests. Burro Series Data Report, UCID-19075-Vol.1, December 1982.
[10] F. Gavelli, E. Bullister, H. Kytomaa, Applications of CFD to LNG spills into geometrically complex environments, J. Hazard. Mater. 159 (2008) 158–168.
[11] T.C. Brown et al., Falcon Series Data Report, 1987 LNG Vapor Barrier Verification Field Trials, Report No. GRI-89/0138, June 1990.
[12] J.C. Tannehill, D.A. Anderson, R.H. Pletcher, Computational Fluid Mechanics and Heat Transfer, second ed., Taylor & Francis, Philadelphia, Pennsylvania, 1997, pp. 313–317.
[13] 49 CFR 193.2059(b)(2).
[14] D. Golder, Relations among stability parameters in the surface layer, Bound Layer Meteorol. 3 (1972) 47–58.
[15] A. Luketa-Hanlin, R.P. Koopman, D.L. Ermak, On the application of computational fluid dynamics codes for liquefied natural gas dispersion, J. Hazard. Mater. 140 (2007) 504–517.
[16] G.F. Carey, Computational Grids, Generation, Adaptation, and Solution Strategies, Taylor & Francis, Washington, DC, 1997, pp. 150–153.
[17] NFPA 59A-2001 section 2.2.3.3 as referenced by 49 CFR 193.2059.